Ind. J. Pharm. Edu. Res., 2027; 61:10.5530/ijper.20270038.
https://www.ijper.org

Original Article

Fabrication and Optimization of Dual Drug-Loaded Itraconazole-Quercetin PCL/PVP Electrospun Nanofibers for Post-Surgical Skin Cancer Therapy

Priya Palanisamy*, Allimalarkodi Shanmugham*, Venkatesh Aditiyaa Narayana, Sambath Kumar Ramanadhan

Department of Pharmaceutics, The Erode College of Pharmacy, The Tamil Nadu Dr. M.G.R. Medical University, Tamil Nadu, INDIA.

ABSTRACT

Objectives: The objective of the study was to design, optimize, and evaluate dual drug-loaded itraconazole and quercetin PCL/PVP nanofibers for sustained localized delivery in the post-surgical management of skin cancers. Residual tumour cells, oxidative stress, and delayed wound healing are challenges in the post-surgical management of skin cancer. Itraconazole is a triazole antifungal drug that has anti-angiogenic and Hedgehog signaling inhibitory activity, and quercetin is a flavonoid that has antioxidant and pro-apoptotic activity. Both drugs are poorly soluble in water, and have low oral bioavailability making a nanofiber-based drug delivery system suitable for targeted anticancer therapy. **Materials and Methods:** A Box-Behnken Design was used to optimize nanofiber fabrication using a PCL/PVP blend in chloroform/DMF solution, with voltage, flow rate, and PCL:PVP ratio as independent variables, and fiber diameter, encapsulation efficiency, and cumulative drug release as dependent variables. Characterization of optimized formulation was done by FTIR, DSC, XRD and SEM and it's *in vitro* drug release, release kinetics, physical stability, antioxidant activity, and cytotoxicity against A431 cells was evaluated. **Results:** The optimized formulation (voltage 17.0 kV, flow rate 0.25 mL/h, PCL: PVP 2.29) yielded bead-free, uniform nanofibers with a fiber diameter of 389.8±35.0 nm, encapsulation efficiency of 93.95% (itraconazole) and 92.89% (quercetin), and cumulative drug release of 88.00% (itraconazole) and 87.50% (quercetin) at 8 hr, following the Korsmeyer-Peppas model with non-Fickian (anomalous) transport (n=0.61 and 0.58, respectively). FTIR, DSC, and XRD confirmed amorphous drug dispersion with no chemical incompatibility. The formulation showed a water contact angle of 89.49±0.29° (mildly hydrophilic), potent antioxidant activity (DPPH IC_{50}=158.3 µL), significant cytotoxicity against A431 cells (IC_{50}=520 µg/mL, 24 hr), and remained physically stable for 45 days under both room-temperature and refrigerated storage. **Conclusion:** The dual drug loaded electrospun ITZ/QCT PCL/PVP nanofibrous platform shows synergistic anticancer, antioxidant and stability properties making it a potential localized topical therapy for post-surgical skin cancer management.

Keywords: Box-Behnken Design, Cytotoxicity, Electrospun nanofibers, Itraconazole, PCL/PVP, Quercetin, Skin cancer, Sustained drug release.

Correspondence:
Ms. Priya Palanisamy
Department of Pharmaceutics, The Erode College of Pharmacy, The Tamil Nadu Dr. M.G.R. Medical University, Erode, Tamil Nadu, INDIA.
Email: Priya.p@ecp.ac.in

Dr. Allimalarkodi Shanmugham
Department of Pharmaceutics, The Erode College of Pharmacy, The Tamil Nadu Dr. M.G.R. Medical University, Erode, Tamil Nadu, INDIA.
Email: allimalarkodi1968@gmail.com

Received: 15-05-2026;
Revised: 21-07-2026;
Accepted: 02-09-2026.

INTRODUCTION

The incidence of Skin Cancer (SC) has increased dramatically over the past several decades.[1] Skin cancers can be divided into melanoma and non-melanoma skin cancers, such as basal cell and squamous cell.[2] Therapies available include surgery, chemotherapy, radiation therapy, immunotherapy and molecular targeted therapy as they depend on tumor histology and stage.[3] Surgery is the primary treatment for early stage tumors, but it can lead to scarring, loss of function, and cosmetic issues, particularly in the areas of the body that are sensitive.[4] There is a possibility of recurrence after successful surgery, and many patients are non-responsive, resistant to therapy, or have serious side effects.[5] Local and topical delivery systems enable direct delivery to the tumor location with minimal systemic exposure.[6] The stratum corneum, however, is a barrier to topical vehicles (creams, gels, and ointments) that restricts transdermal efficacy, release, and retention, reducing their effectiveness and compliance.

The high surface-to-volume ratio, tunable porosity, and extracellular-matrix-mimicking structure of electrospun nanofibers have attracted great interest in their application to topical and targeted therapy of skin cancer.[7-9] The nanofibers can be used to encapsulate anticancer drugs and for controlled local delivery, and can have high skin adherence.[10] They take advantage of the stratum corneum barrier by having high surface

DOI: 10.5530/ijper.20270038

Copyright Information :
Copyright Author (s) 2027 Distributed under Creative Commons CC-BY 4.0

Publishing Partner : Manuscript Technomedia. [www.mstechnomedia.com]

area for skin adhesion, a favorable concentration gradient for drug diffusion as well as having nanoscale dimensions that would enhance permeation through skin pores.[11] Electrospinning allows the precise control of fiber composition, morphology and biofunctionalization, providing multi-functional constructs capable of simultaneous delivery of different drugs or photosensitizers and targeting moieties;[12] encapsulation within a nanometric fiber prevents rapid inactivation of the drug by physiological or environmental factors.[13]

The polymers used in this study were Polycaprolactone (PCL) and Polyvinylpyrrolidone (PVP), and the functional molecules were itraconazole and quercetin. PCL is an FDA approved, biodegradable, synthetic polymer that can be dissolved in methanol, acetic acid, chloroform, benzene, trifluoroethanol and dichloromethane.[14] High hydrophobicity and slow degradation are the limitation of its biomedical application; it is biocompatible *in vitro* and *in vivo* and has been blended with water soluble and biocompatible polymers like PVP to enhance its hydrophilicity and biocompatibility. PVP is a hydrophilic polymer that has excellent biocompatibility and low toxicity, has strong adhesion capabilities, and can interact with hydrophilic and hydrophobic materials.[15] PCL and PVP are tissue compatible and non-toxic.[16,17]

Itraconazole is a broad-spectrum triazole antifungal drug which recently has been reported to have anticancer activity due to its antiangiogenic and anti-signaling effects in tumor growth and proliferation.[18,19] Quercetin is a natural polyhydroxy flavone that has antioxidant, antitumoral, antimicrobial and antiviral properties.[17-20] Itraconazole is a BCS Class II drug, with variable oral bioavailability, high plasma protein binding, poor dermal permeability, and a highly variable response to the drug when applied topically.[21] Quercetin is also poorly soluble in water, has a short half-life, is light-sensitive and is rapidly metabolized prior to systemic circulation, thus reducing its stability and availability.[22,23] Hence, an advanced drug delivery system is required for enhancing the solubility, stability, permeability and controlled release of both drugs.

Itraconazole and quercetin could be synergically used for the treatment of cancer and wounds, providing enhanced anticancer and antioxidant properties, when combined in the same nanofibrous matrix to enhance the management of postoperative skin cancers. The delivery of itraconazole and quercetin in PCL/PVP nanofibers for the treatment of post-surgical skin cancer has not been extensively explored. The main goal of this study was to design, optimize and evaluate dual drug-loaded PCL/PVP nanofibers to be prepared using a Box-Behnken experimental design. The formulations were morphologically characterized, thermally evaluated, and assessed for crystallinity, wettability and drug release kinetics, followed by their *in vitro* antioxidant activity and cytotoxicity against A431 human epidermoid carcinoma cells, which proved them to be suitable as a sustained release localized therapeutic platform for managing post-surgical skin cancer treatment. Although individual studies on itraconazole and quercetin nano formulations have been reported, there is no previous work that has combined both agents in a single electrospun PCL/PVP nanofiber system optimized using Box-Behnken Design for the localized, sustained post-surgical delivery targeting residual tumour cells and oxidative stress simultaneously.

MATERIALS AND METHODS

Materials

Itraconazole ($C_{35}H_{38}Cl_2N_8O_4$) and quercetin ($C_{15}H_{10}O_7$) were procured as pharmaceutical-grade substances. Polycaprolactone (PCL, Mw ~9000-11000 Da) and Polyvinylpyrrolidone (PVP K30) were obtained from Sigma-Aldrich. Chloroform ($CHCl_3$) and Dimethylformamide (DMF) (C_3H_7NO) were of analytical reagent grade. Phosphate buffer saline (pH 7.4) was prepared in the laboratory. A431 human epidermoid carcinoma cells were procured from the National Centre for Cell Science (NCCS), Pune, India. All other reagents were of analytical grade and used without further purification.

Preformulation Studies

Determination of λ_{max}

The λ_{max} of itraconazole and quercetin was determined by measuring the standard solution of both compounds (10 µg/mL) using a UV-visible spectrophotometer with a wavelength range of 200 to 400 nm. For this purpose, the standard solutions of both drugs were prepared in chloroform and DMF, respectively. It is important to mention here that the respective solvents served as the blanks.

Calibration Curve

Calibration curves for itraconazole and quercetin were prepared by dissolving 10 mg of each drug separately itraconazole in 1 mL of chloroform and quercetin in 1 mL of DMF and making up to 10 mL with phosphate buffer to obtain stock solutions of 1000 µg/mL each. From each stock solution, 1 mL was pipetted and diluted to 100 mL with phosphate buffer to yield intermediate solutions of 10 µg/mL. Aliquots of 2, 4, 6, 8, and 10 mL from each intermediate solution were transferred into separate 10 mL volumetric flasks and made up to the mark with phosphate buffer, giving working standard concentrations ranging from 2 to 10 µg/mL. Absorbance of itraconazole solutions was determined at λ_{max} of 262 nm and quercetin solutions at λ_{max} of 374 nm with the UV-vis Spectrophotometer using phosphate buffer as blank. Calibration curves were plotted between absorbance and concentration and the linearity was verified by obtaining regression equations and correlation coefficients with linear regression analysis (r^2).[24,25]

Compatibility Study (FTIR)

To evaluate the chemical compatibility and identify possible interactions, Fourier Transform Infrared (FTIR) spectroscopy was used with a Shimadzu FTIR spectrophotometer (ATR mode), ranging from 4000-400 cm^{-1} for pure drugs, individual polymers, physical mixtures (binary and multicomponent), and the final nanofiber formulation.

Preparation of Nanofibers

Preparation of Polymeric Solution

The polymeric solution was prepared by appropriate amount of Polycaprolactone (PCL) (0.84 g) was dissolved in chloroform (7 mL) under magnetic stirring of 400-500 rpm, controlled temperature of 30-40°C, for 1-2 hr until a clear and homogeneous solution was obtained. Under similar stirring conditions, 0.36 g of Polyvinylpyrrolidone (PVP) was completely dissolved in 3 mL of Dimethylformamide (DMF) after 15-30 min. Once the polymers had completely dissolved, itraconazole was added into the PCL solution and stirred to complete dissolution. Simultaneously, quercetin was dissolved in DMF and added to the PVP solution while stirring. The PVP-quercetin solution was slowly added to the PCL-itraconazole solution, stirred for 3 hr at 400-500 rpm at 30-40°C, and formed a clear and uniform viscous solution appropriate for electrospinning. The preparation of the polymeric solution is illustrated in Figure 1.

Electrospinning of nanofibers

The prepared polymeric solution was allowed to cool to room temperature and kept undisturbed for 30 min to ensure stabilization and removal of air bubbles. The solution was then transferred into a 10 mL syringe equipped with a 24-gauge needle. The electrospinning process was performed at an applied voltage of 17-19 kV and a controlled flow rate of 0.25 mL/hr. The distance between the needle tip and the collector was maintained at 15 cm. The collector was covered with aluminum foil to facilitate easy collection of nanofibers. The electrospinning process was continued for approximately 3 hr, after which the formed nanofibers were collected from the surface of the collector and stored for further characterization.[26] A schematic representation of the electrospinning setup is shown in Figure 1.

Experimental Design and Optimization

The formulation optimization was done through three factor and three level Box-Behnken design, which was generated by Design-Expert® 13 software. The variables considered were the applied voltage (A: 12-18 kV), flow rate (B: 0.25-0.50 mL/hr) and the PCL:PVP ratio (C: 2.0-2.7). The responses were the diameter of the fibers (Y1: minimize), efficiency of encapsulation (Y2: maximize) and percentage drug release after 8 hr (Y3: maximize). The number of experimental runs generated was seventeen with five center point replicates. The data were fitted into a second order polynomial equation and analyzed using ANOVA (Design-Expert® 13). The independent variables and their coded levels used in the Box-Behnken Design are shown in Table 1.

Characterization

Morphological study

Scanning electron microscopy was used to characterize the morphology of the electrospun nanofiber scaffolds. Surface morphology and fiber diameter were evaluated using a ZEISS field-emission SEM. Samples were sputter-coated with gold under argon atmosphere and imaged at 10.00 kV, 11.0 mm working distance, at magnifications of 10,000×-45,000×. Fiber diameters were measured from three independent measurements using the ZEISS measurement tool.

Differential Scanning Calorimetry (DSC)

The DSC of pure components revealed the polymorphic transition (155.0°C) and melting endotherm (168.2°C) of itraconazole, the dehydration endotherm (105.3°C) and melting endotherm (320.4°C) of quercetin, the semicrystalline melting peak (60.3°C, ΔHf=−81.5 J/g) of PCL, and the glass transition (~170°C) without melting of PVP K30 which is amorphous. For the drug-polymer interaction, the PCL peak was broadened and suppressed (107.80°C) in the ITZ/QCT-loaded nanofibers, confirming the amorphous solid dispersion formation, while both drug melting peaks were completely absent. The Purity analysis results confirmed enhancement in formulation integrity (99.34 mol%) without degradation during electrospinning, which led to improved solubility and dissolution (Table 5 and Figure 7).[27,28]

X-ray Diffraction (XRD)

Crystalline state and phase identification of pure drugs, polymers and nanofiber formulation were assessed using a PANalytical X'PERT PRO diffractometer equipped with Cu Kα radiation (λ=1.54060 Å) at 40 kV and 10 mA. Samples were scanned over a 2θ range of 10°-80° with a step size of 0.017° 2θ at a scan speed of 5.715 s/step. Peak positions, d-spacing values, and relative crystallinity index were analyzed using HighScore Plus software.[27,28]

Contact Angle Measurement

Water contact angles were measured by the sessile drop method using a goniometer equipped with a digital camera. Deionized water droplets (5 µL) were deposited on 2 × 2 cm nanofiber specimens and contact angles recorded immediately. Three independent measurements were taken and averaged.[29]

Encapsulation Efficiency

Encapsulation efficiency was determined in triplicate (n=3), and the results are expressed as mean±Standard Deviation (SD). Encapsulation Efficiency (EE%) is the fraction of entrapped drug loaded in the nanofiber matrix compared to the amount of drug

added to the formulation during nanofiber fabrication. The drug loaded nanofibers (10 mg) were dissolved in phosphate buffer (pH 7.4) with gentle stirring of 10 mL. The solution was filtered through Whatman filter paper No. 1 and 1 mL of the clear filtrate was diluted to 100 mL using phosphate buffer (100× dilution). Absorbance was measured spectrophotometrically using a UV-visible spectrophotometer (Shimadzu UV-1800, Japan) at 262 nm (Itraconazole) and 374 nm (Quercetin). Concentration of drugs was determined by fitting calibration equations (y=0.031x [ITZ, R^2=0.999] and y=0.059x [QCT, R^2=0.999]), and the total amount of drug recovered was calculated (mg). Encapsulation efficiency was calculated as:[27,28]

$$\% \text{ Encapsulation Efficiency} = \frac{\text{Amount of drug encapsulated}}{\text{Total amount of Drug Added}} \times 100$$

In vitro Drug Release

The *in vitro* release of the drug from nanofiber formulations was determined using the Franz diffusion cell with a 0.45 µm cellulose acetate membrane that was soaked in glycerol for 12 hr. The receptor chamber was filled with 60 mL of phosphate buffer (pH 7.4) at 37±0.5°C with stirring (50-100 rpm). Nanofiber formulation (10 mg) was placed on the membrane in the donor compartment. Samples (1 mL) were taken at 0, 0.5, 1, 2, 3, 4, 5, 6, 7 and 8 hr and replaced with fresh buffer to ensure the sink conditions remained.

Samples were withdrawn (1 mL) and placed immediately into 10 mL volumetric flasks and diluted to the mark with the phosphate buffer (pH 7.4), giving a dilution of 10×. Absorbance values of

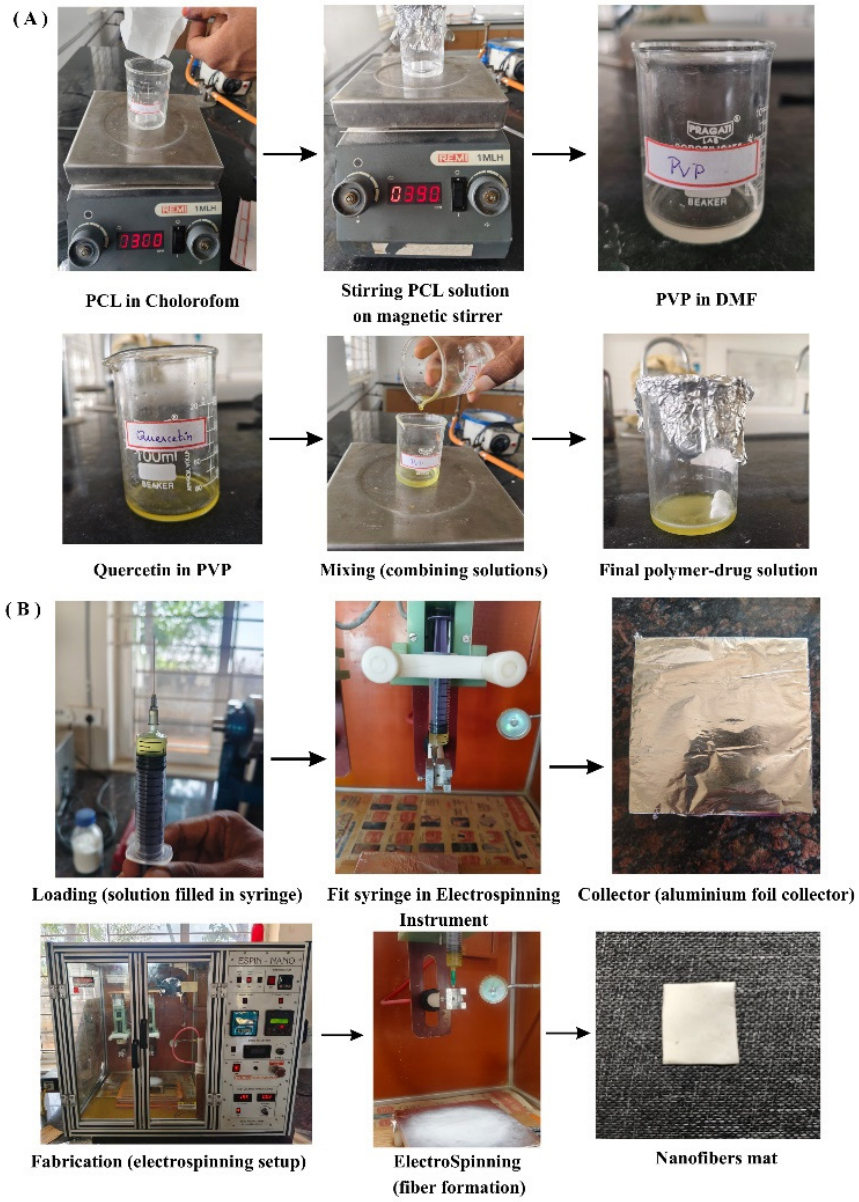


Figure 1: Fabrication of ITZ/QCT-loaded PCL/PVP electrospun nanofibers: (a) preparation of the PCL-itraconazole and PVP-quercetin polymeric solution blend; (b) schematic of the electrospinning setup (applied voltage 17-19 kV, flow rate 0.25 mL/h, 15 cm tip-to-collector distance, aluminium foil collector) used to fabricate the nanofibers.

Table 1: Box-Behnken Design: Independent variables and their coded levels.

Factor	Symbol	Low (−1)	Mid (0)	High (+1)
Voltage (kV)	A	12	15	18
Flow Rate (mL/hr)	B	0.25	0.375	0.50
PCL: PVP Ratio	C	2.0	2.35	2.7

Table 2: Calibration data for Itraconazole and Quercetin.

Conc. (µg/mL)	ITZ Absorbance (262 nm)	QCT Absorbance (374 nm)
0	0.000	0.000
2	0.061	0.115
4	0.123	0.239
6	0.185	0.353
8	0.248	0.478
10	0.311	0.591

diluted samples of Itraconazole and Quercetin were determined using the double-beam UV-visible spectrophotometer at λ_{max}=262 nm and 374 nm with phosphate buffer as blank, respectively. Drug concentrations were determined using previously validated calibration equations and Cumulative percentage Drug Release (%CDR) was calculated with appropriate correction for volume replacement at each sampling time point. The optimized formulation. The release kinetics were analysed by DDSolver 1.0 (Zero-order, First-order, Higuchi and Korsmeyer-Peppas models).[28]

Physical Stability Study of Quercetin-Itraconazole Loaded Nanofibers

The optimized nanofiber formulation was packaged in airtight containers and kept at the refrigerated temperature (4-6°C) and room temperature (25°C/65±5% RH (Relative Humidity)). The physical appearance and the morphology of samples was determined by Scanning Electron Microscopy (SEM) and the percentage of Encapsulation Efficiency (EE%) for quercetin and itraconazole was determined on Day 0 and Day 45. The study was conducted to evaluate the physical stability of nanofibers for different storage conditions.[29]

Antioxidant Activity (DPPH ASSAY)

The free radical scavenging activity of nanofibers was performed using the DPPH (1,1-diphenyl-2-picrylhydrazyl) assay. A freshly prepared 0.1 mM DPPH solution in methanol was added to serial dilutions of the formulation (50-250 µL) and ascorbic acid (1 mg/mL) as a positive control. The reaction solutions were kept in the dark at room temperature for 30 min and absorbance was read at 517 nm on a UV-vis spectrophotometer with methanol as blank. The percentage inhibition of DPPH radicals was determined according to the following equation: % Inhibition= [(Ac − As) / Ac] × 100. IC_{50} was calculated based on linear regression of the concentration versus % inhibition graph.

Cytotoxicity Assay

The cell toxicity of ITZ/QCT co-loaded nanofibers was evaluated using MTT assay, which is based on the activity of mitochondrial dehydrogenase, as an indicator of cell viability. The A431 cells (NCCS, Pune) were cultured in the medium MEM containing 10% FBS, 1% sodium bicarbonate, 1% nonessential amino acids, and 1% sodium pyruvate at 37°C, humidified 5% CO_2, and subcultured at 70-80% confluency. The nanofiber mat was dissolved in sterile DMSO to give stock concentrations of 100-1000 µg/mL (DMSO <0.1% v/v). 24 hr cells cultured in 96 well plate treated with the compound 24 hr, then MTT (0.5 mg/mL) added for 5 hr; formazan crystals dissolved in DMSO and absorbance read at 570/650 nm to determine viability and IC_{50}.

The percentage cell viability was determined by:

$$\% \text{ Cell Viability} = \frac{\text{Absorbance of treated cells}}{\text{Absorbance of control cells}} \times 100$$

The dose-response curve was used to graphically determine the IC_{50} with GraphPad Prism software.

Ethical statement

No human participants or experimental animals were involved in this study. The A431 human epidermoid carcinoma cell line was procured from the National Centre for Cell Science (NCCS), Pune, India, and all experimental procedures complied with institutional laboratory biosafety guidelines.

Statistical analysis

Statistical analysis was performed using Design-Expert® version 13.0 software for optimization and GraphPad Prism version 9.0 for cytotoxicity analysis. Experimental data were expressed as mean±Standard Deviation (SD) from triplicate measurements (n=3). Analysis of Variance (ANOVA) was used to determine the significance of model terms, and p<0.05 was considered statistically significant. Box-Behnken design were analysed using Design-Expert® software. Quadratic polynomial models were generated and evaluated by Analysis of Variance (ANOVA). Model adequacy was assessed using the F-value, p-value, coefficient of determination (R^2), adjusted R^2, predicted R^2,

adequate precision, Coefficient of Variation (CV), and lack-of-fit test. Statistical significance was considered at $p<0.05$.

RESULTS

λ_{max} Determination and Calibration Curve

UV spectral scanning established λ_{max} at 262 nm for itraconazole (chloroform; principal peak at 262.00 nm, absorbance 0.571; secondary peak at 236.50 nm) and at 374.5 nm for quercetin (DMF; Band I cinnamoyl system at 374.50 nm, absorbance 0.638; Band II benzoyl system at 256.50 nm, absorbance 0.668), consistent with the characteristic two-band flavonoid UV absorption profile. Calibration curves exhibited excellent linearity (Beer-Lambert law compliance): ITZ: y=0.031x, R^2=0.999; QCT: y=0.059x, R^2=0.999, over 0-10 µg/mL. The UV-visible absorption spectra of itraconazole and quercetin are presented in Figure 2. The calibration data for itraconazole and quercetin are presented in Table 2.

FTIR Compatibility Studies

FTIR spectra of pure itraconazole revealed characteristic N-H/O-H stretching at 3383.47 cm^{-1}, C=O stretching of piperazinone ring at 1696.05 cm^{-1}, C-N stretching of triazole ring at 1329.84 cm^{-1}, and C-O-C stretching of dioxolane ring at 1223.57 and 1044.05 cm^{-1}. Pure quercetin exhibited phenolic O-H stretching at 3275.77 cm^{-1}, C=O ketone stretching at 1660.14 cm^{-1}, and aromatic C=C stretching at 1602.70 and 1507.91 cm^{-1}. PCL showed characteristic ester C=O stretching at 1723.33 cm^{-1} and PVP displayed lactam C=O stretching at 1642.91 cm^{-1}.

Physical mixture spectra of all components demonstrated co-existence of characteristic peaks from all individual ingredients without appearance of new peaks or significant peak shifts, confirming absence of chemical incompatibility. The nanofiber formulation spectrum retained the PCL ester C=O at 1726.20 cm^{-1}, PVP lactam C=O at 1654.40 cm^{-1}, and ITZ C=O at 1586.90 cm^{-1}, with no new peaks, confirming physical compatibility and successful drug encapsulation without chemical interaction during electrospinning.[25,30-32] The FTIR spectra of pure drugs, polymers, physical mixtures, and optimized nanofibers are shown in Figure 3.

Box-Behnken Design optimization of Itraconazole-quercetin Loaded Pcl/Pvp Electrospun Nanofibers

A three-factor, three-level Box-Behnken Design (BBD) employing Design-Expert® 13 software generated 17 experimental runs spanning the design space defined by voltage (12-18 kV), flow rate (0.25-0.50 mL/hr), and PCL:PVP ratio (2.00-2.70 mg). Across these runs, fiber diameter ranged from 391.9 to 397.8 nm, encapsulation efficiency from 91.0 to 94.2%, and drug release from 84.8 to 88.4% (Table 3), confirming a wide and informative response surface across the selected factor ranges. Centre-point replicates (Runs 9-13 corresponding to Std 5, 8, 15, 16, 17) showed

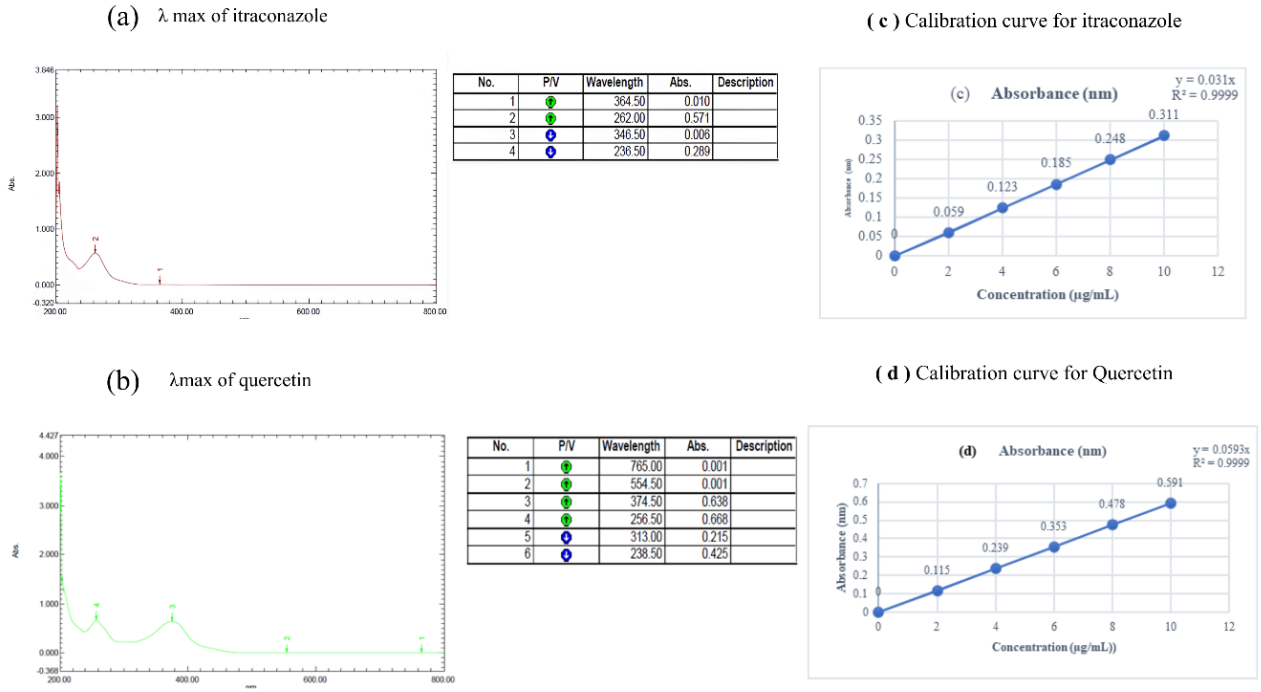


Figure 2: UV-visible absorption spectra of (a) Itraconazole (ITZ) in chloroform showing λ_{max} at 262 nm and (b) Quercetin (QCT) in DMF showing λ_{max} at 374.5 nm and Calibration curve of itraconazole (c) and Quercetin (d).

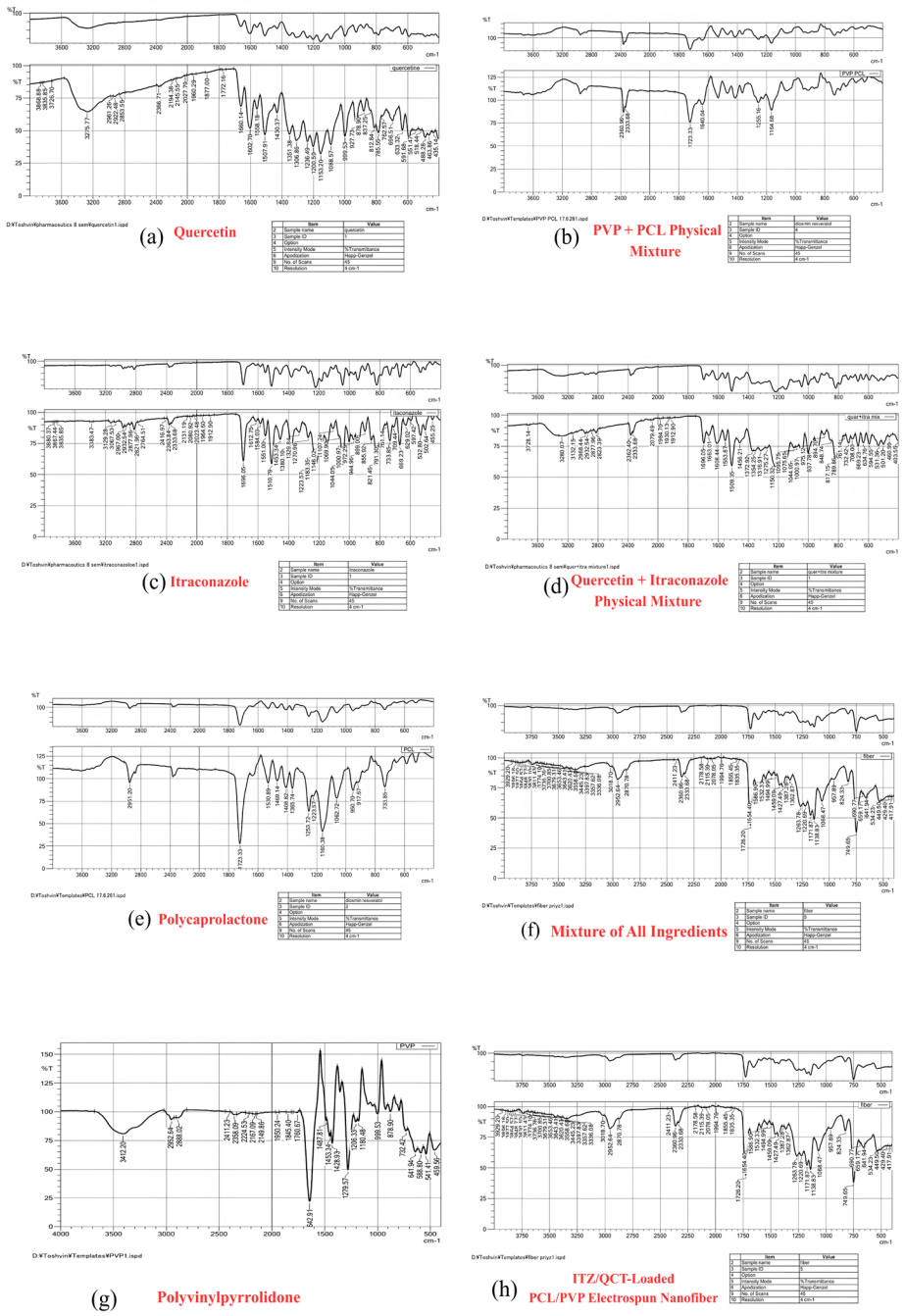


Figure 3: FTIR spectra (4000-400 cm^{-1}) of pure drugs (a) itraconazole, (c) quercetin, polymers (e) PCL, (g) PVP, physical mixtures (b, f), and (h) the ITZ/QCT-loaded PCL/PVP nanofiber formulation, showing retention of the characteristic component peaks listed in Section 3.2 without new peak formation.

low variability, supporting the reproducibility and adequacy of the experimental model.

ANOVA and Model Statistics

All three response models were highly significant ($p<0.0001$). Flow rate (B) was determined to be the most important variable influencing all three responses ($p<0.0001$), where increase in flow rate leads to an increase in diameter of the fibers but reduction in encapsulation efficiency and drug release rate. The effect of PCL:PVP ratio (C) was highly significant on all three responses, whereas the effect of applied voltage (A) was significant on fiber diameter only. Interaction between BC was significant in all three responses, suggesting a synergistic interaction of flow rate and composition of the polymers. Quadratic effects were significant on EE and drug release models, and hence, quadratic models had to be used. The model fit statistics obtained from ANOVA are summarized in Table 3.

The high R^2 values (≥0.9669 for all responses) indicated that over 96% of response variation was explained by the respective models. The strong agreement between adjusted R^2 and predicted

R^2 (difference<0.2) confirmed absence of overfitting. Adequate precision values well above 4 confirmed a sufficient signal to noise ratio for design space navigation is reliable.

The effect of the three independent variables on the response was quantified by obtaining a regression equation for each response in the Design-Expert® software. The regression equations can give information about the effect of the independent variables like the voltage (A), flow rate (B) and PCL:PVP ratio (C).

Y_1: Fiber Diameter (2FI Model)

$$Y1 = 394.17 - 0.3243A + 1.29B + 0.8970C + 0.1519AB + 0.0715AC + 1.24BC$$

Interpretation

Flow rate (B) and PCL:PVP ratio (C) were found to be positive factors affecting the fiber diameter while voltage (A) was negative factor. The most significant factor was the flow rate, followed by the polymer ratio. The BC interaction was highly significant, the AB interaction was not significant and the AC interaction was not significant, verifying the appropriateness of the 2FI model.

Y_2: Encapsulation Efficiency (Quadratic Model)

$$Y2 = 92.86 + 0.0792A - 0.6738B - 0.5517C + 0.0479AB - 0.1615AC - 0.3309BC - 0.0324A^2 + 0.3308B^2 - 0.2403C^2$$

Interpretation

Flow rate (B) and PCL:PVP ratio (C) significantly affected the encapsulation efficiency with the flow rate having the most significant effect. The voltage (A) had a small and insignificant positive effect. There were significant AC and BC interactions which further reduced EE, and significant quadratic terms (A^2, B^2, and C^2) that gave justification to the quadratic model.

Y_3: Drug Release (Quadratic Model)

$$Y3 = 87.48 + 0.0373A - 0.6658B - 0.6402C - 0.0081AB - 0.1538AC - 0.5617BC - 0.0677A^2 + 0.0644B^2 - 0.1630C^2$$

Interpretation

Flow rate (B) and PCL:PVP ratio (C) showed significant reduction in drug release, while voltage (A) did not significantly affect the drug release alone. The BC interaction was the strongest negative

Table 3: Model fit statistics for all three responses.

Parameter	Fiber Diameter (nm)	EE (%)	Drug Release (%)
Model Type	2FI	Quadratic	Quadratic
R^2	0.9669	0.9938	0.9889
Adjusted R^2	0.9470	0.9859	0.9746
Predicted R^2	0.8162	0.9743	0.8384
Adequate Precision	22.911	35.179	24.538
C.V. (%)	0.1011	0.1235	0.2029
Lack of Fit (p)	0.4193 (NS)	0.9539 (NS)	0.2010 (NS)

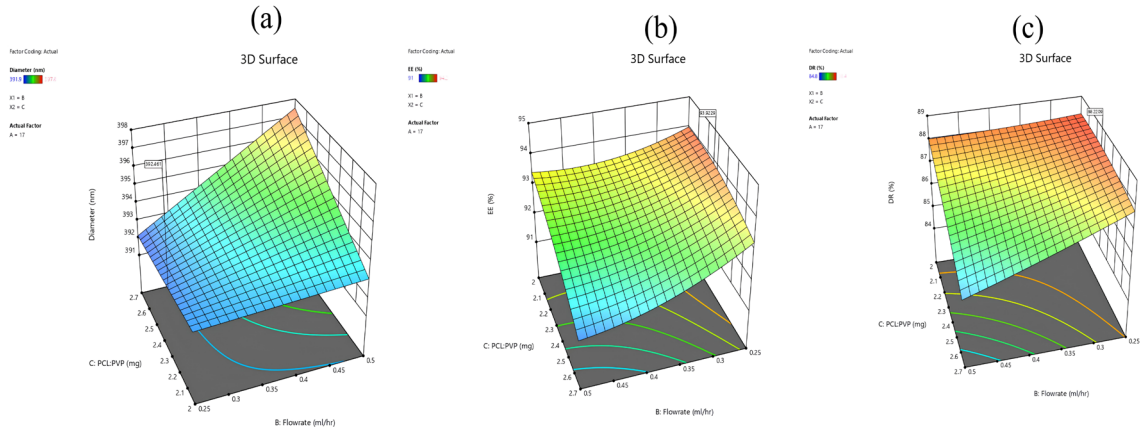


Figure 4: Three-dimensional Box-Behnken response surface plots showing the combined effect of applied voltage, flow rate, and PCL:PVP ratio on (a) fiber diameter, (b) encapsulation efficiency, and (c) cumulative drug release at 8 hr.

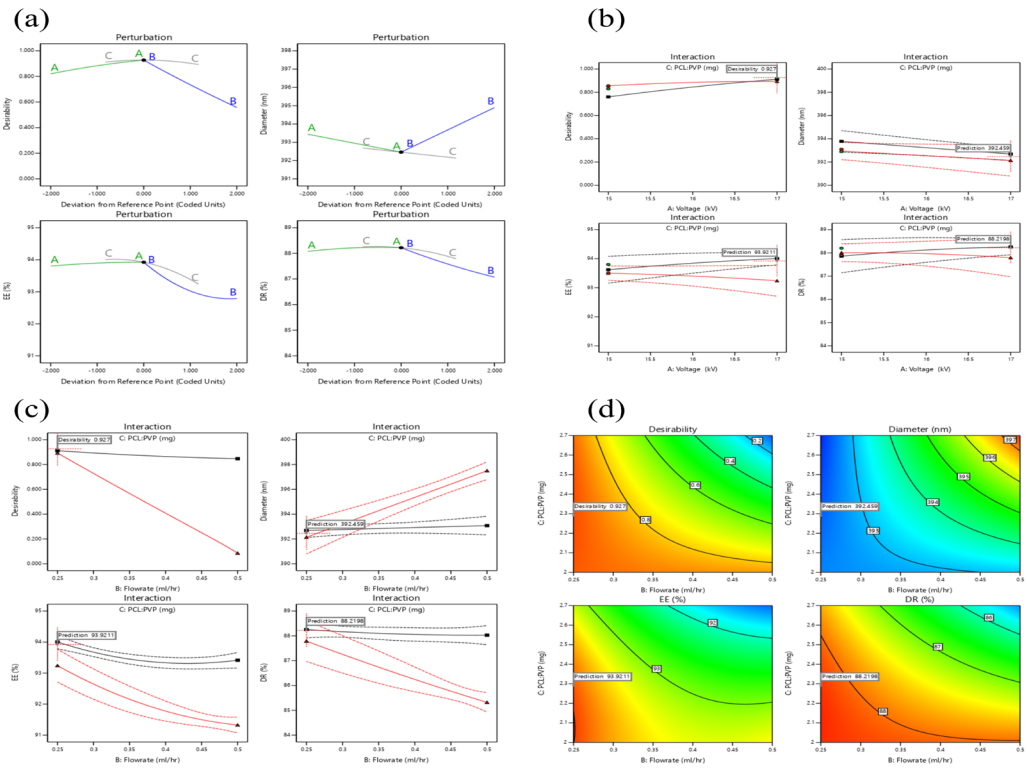


Figure 5: Design-Expert® diagnostic plots for the optimized Box-Behnken model: (a) perturbation plots showing the individual effect of each factor on the three responses; (b, c) two-factor interaction plots for the flow rate × PCL:PVP ratio (BC) and voltage × PCL:PVP ratio (AC) interactions; (d) two-dimensional contour plot showing the optimal design space (high voltage, low flow rate, low PCL:PVP ratio).

Table 4: Numerical optimization constraints and the resulting optimized formulation parameters (voltage, flow rate, PCL:PVP ratio) and predicted responses (fiber diameter, encapsulation efficiency, drug release) for the top-ranked solution (composite desirability D=0.927).

Parameter	Optimized Value	Goal
A: Voltage (kV)	17.00 kV	In range
B: Flow Rate (mL/hr)	0.250 mL/hr	In range
C: PCL: PVP Ratio	2.290	In range
Y1: Fiber Diameter (nm)	392.459 nm	Minimize
Y2: Encapsulation Efficiency (%)	93.921%	Maximize
Y3: Drug Release (%)	88.220%	Maximize
Overall Desirability	0.927	—

interaction, followed by the AC interaction, which suggested that both flow rate and polymer ratio had an interaction effect on the drug release. The high value of the A^2 term was significant, indicating curvature in the response and thus validating the quadratic model.

Response Surface Analysis

The combined effects of voltage, flow rate, and PCL:PVP ratio on each of the responses were shown in three-dimensional response surface plots (Figure 4). The flow rate and PCL:PVP ratio showed an increase in fiber diameter (391.9-397.8 nm) due to increased delivery of polymer and solution viscosity in the presence of strong electrostatic force. The results of EE indicated that the surface was concave at low voltage and low flow rate and PCL:PVP ratio, and that the surface was dome-shaped at high voltage and high flow rate and PCL:PVP ratio because the viscous overloading effect and incomplete solvent removal effect affected the stability of the encapsulation interface. The release of the drug was greater for higher voltage but lower for higher flow rate and lower PCL:PVP ratio, because thicker and less porous membranes prevented diffusion and less cumulative release of the drug.

Perturbation, Interaction, And Contour Plot Analysis

Perturbation plots revealed that flowrate was the most significant factor for fiber diameter, encapsulation efficiency, and drug release while PCL:PVP ratio had the strongest influence on the three responses due to its effect on solution viscosity, fiber formation, and drug entrapment. The interaction plots showed that there were synergistic and quadratic interactions for flowrate, PCL:PVP ratio and voltage for all responses, with BC (flowrate × PCL:PVP ratio) being most significant and AC (voltage × PCL:PVP ratio) being significant for encapsulation efficiency and drug release. The optimum region (high voltage, low flowrate, low PCL:PVP ratio) was verified by contour plots, which showed the

nonlinear variable interactions and confirmed the Box-Behnken design (Figure 5).

Numerical Optimization and Validation

A numerical optimization was performed simultaneously considering minimum fiber diameter, maximum EE, and maximum drug release within the range (all desirable) that yielded 76 feasible solutions. The top-ranked optimal formulation with composite desirability D=0.927 was identified at Voltage=17.0 kV, Flow Rate=0.25 mL/hr, and PCL: PVP=2.29, predicting Diameter=392.459 nm, EE=93.921%, and DR=88.220%. The optimized formulation parameters obtained from numerical optimization are presented in Table 4.

The optimized formulation was experimentally prepared and characterized, and was found to be having fiber diameter of 389.8±35.0 nm, EE of 93.95% (ITZ) and 92.89% (QCT) and cumulative drug release of 88.00% (ITZ) and 87.50% (QCT) at 8 hr. The BBD-RSM models showed high predictive accuracy and validity for formulation scale up as indicated by the high correlation between the predicted and experimental values (prediction error<1.5%).

Scanning Electron Microscopy

The optimized nanofibers showed a well-dispersed and randomly oriented fibrous matrix with smooth and continuous fibre morphology, which confirmed that there was no drug aggregation or precipitation in the polymer matrix. A porous interconnected structure was observed at 10,000×, which facilitated moisture balance and long-term drug permeation. At higher magnifications (20,000×-25,000×), ribbon-like or flattened fiber morphology

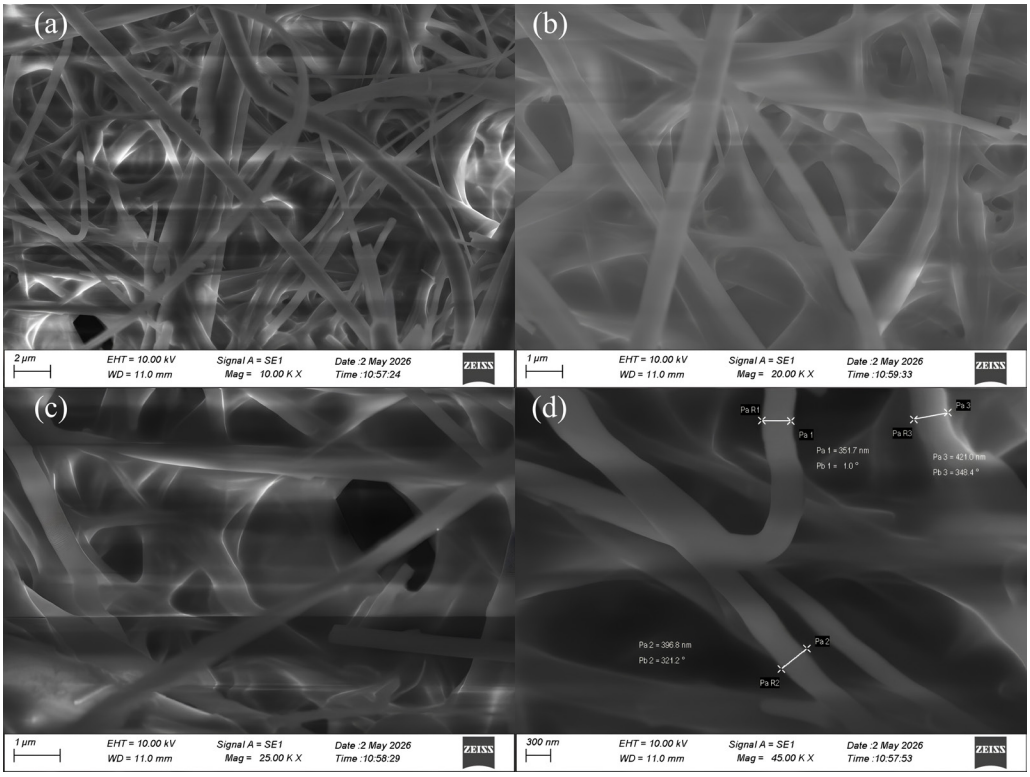


Figure 6: SEM micrographs of the optimized ITZ/QCT-loaded PCL/PVP nanofibers at (a) 10,000×, (b) 20,000×, (c) 25,000×, and (d) 45,000× magnification (Zeiss field-emission SEM, gold sputter-coated), showing smooth, bead-free, randomly oriented fibers with a mean diameter of 389.8±35.0 nm (*n*=3).

Table 5: Summary of DSC thermal parameters for pure components and nanofiber formulation.

Sample	Tg (°C)	Tm (°C)	ΔHf (J/g)	Key Observation
Pure Itraconazole	—	168.2	—	Crystalline; polymorphic transition at 155°C
Pure Quercetin	—	320.4	—	Crystalline; dehydration at 105.3°C
Pure PCL	~−60	60.3	−81.5	Semicrystalline; sharp endotherm
PVP K30	~170	None	—	Amorphous; hygroscopic Tg
Nanofiber Formulation	~170 (PVP)	313.72	93.12	No drug peaks; amorphous dispersion confirmed

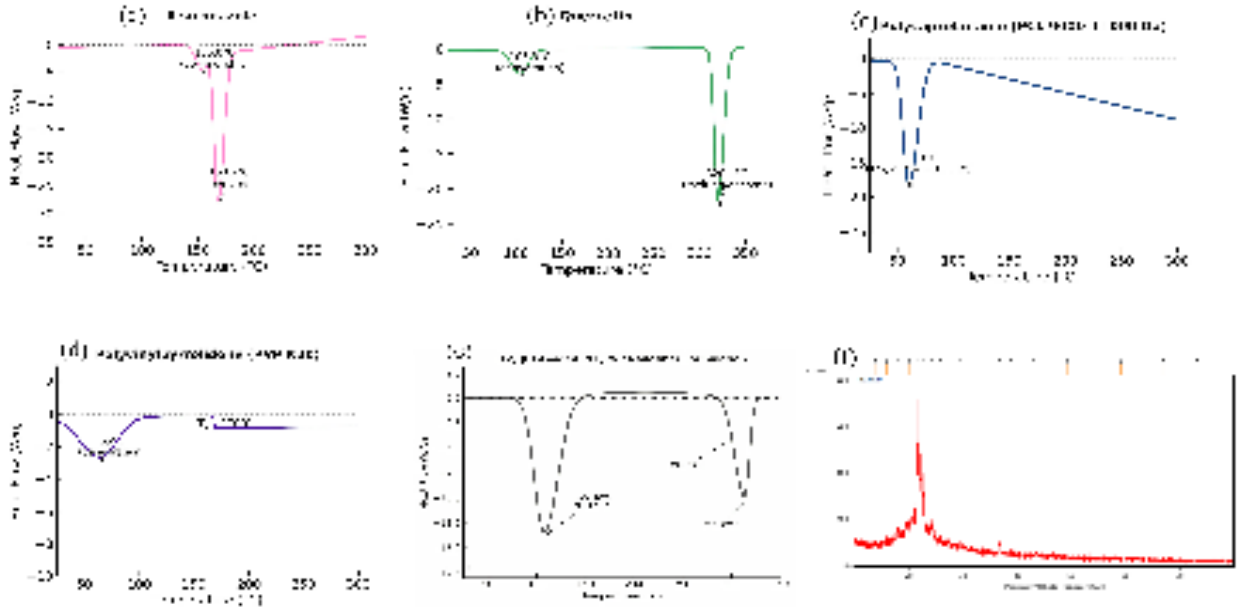


Figure 7: DSC thermograms (25-350°C, 10°C /min, N2 purge) of (a) pure itraconazole, (b) pure quercetin, (c) PCL, (d) PVP K30, and (e) the optimized ITZ/QCT-loaded PCL/PVP nanofiber formulation, showing disappearance of both drug melting endotherms in the formulation. XRD diffractograms of pure drugs, polymers, and ITZ/QCT-loaded nanofiber formulation.

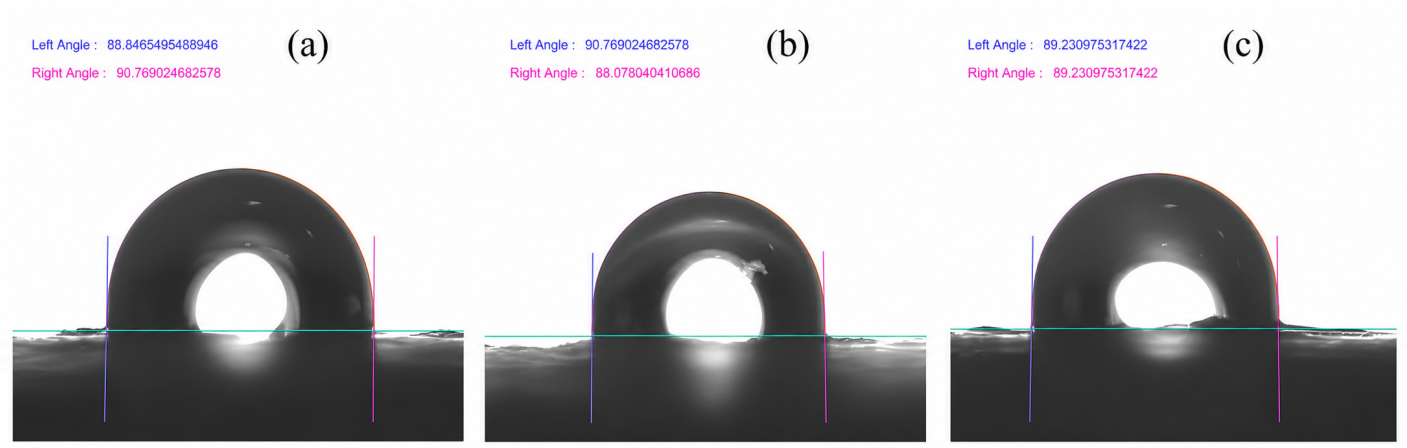


Figure 8: Water contact angle (sessile drop method, 5 µL deionized water droplets) of the optimized ITZ/QCT-loaded PCL/PVP nanofiber membrane on three independent samples (89.82°, 89.42°, 89.23°), mean=89.49±0.29°, indicating a mildly hydrophilic surface (contact angle < 90°).

was seen, which was typical of PCL-PVP electrospun systems and was thought to come from the differential evaporation of the solvent during fiber formation. At high magnification (45,000×), precise fiber diameter measurements yielded Pa1=351.7 nm, Pa2=396.8 nm, and Pa3=421.0 nm, giving a mean fiber diameter of 389.8±35.0 nm (n=3), which is close to the value predicted by BBD-RSM (392-394 nm). High surface area and sub-400 nm diameter are predicted to improve drug dissolution and maintain localized drug delivery at the wound interface. The surface morphology of the optimized nanofibers was examined by SEM (Figure 6).

Differential Scanning Calorimetry

DSC thermograms of pure components showed characteristic events: itraconazole exhibited a polymorphic transition at 155.0°C and a sharp crystalline melting endotherm at 168.2°C; quercetin displayed a dehydration endotherm at 105.3°C and a sharp melt at 320.4°C; PCL showed a single sharp semicrystalline melting peak at 60.3°C (ΔHf=−81.5 J/g); and PVP K30 exhibited a glass transition at ~170°C with no melting endotherm, confirming its fully amorphous character.

In the ITZ/QCT-loaded PCL-PVP nanofiber formulation, the characteristic melting peaks of both itraconazole (168.2°C) and quercetin (320.4°C) were completely absent, providing unequivocal evidence of amorphous solid dispersion formation. The PCL melting peak was broadened and suppressed (107.80°C), indicating disruption of the polymer crystalline lattice by drug-polymer interactions. Purity analysis confirmed formulation integrity at 99.34 mol%, with no evidence of drug

Table 6: Contact angle measurements of optimized ITZ/QCT-loaded PCL/PVP nanofiber formulation (*n*=3).

Measurement	Left Angle (°)	Right Angle (°)	Average (°)
Sample 1	88.87	90.77	89.82
Sample 2	90.77	88.08	89.42
Sample 3	89.23	89.23	89.23
Overall Mean±SD	—	—	89.49±0.29

Table 7: Encapsulation efficiency of itraconazole- and quercetin-loaded optimized electrospun PCL: PVP nanofibers prepared in three independent batches (mean±SD, *n*=3).

Batch	Itraconazole EE (%)	Quercetin EE (%)
Batch 1	93.57	92.47
Batch 2	93.95	92.89
Batch 3	94.33	93.31
Mean±SD	93.95±0.38	92.89±0.42

degradation during electrospinning. Conversion of crystalline drugs to amorphous dispersions within the polymer matrix is expected to substantially enhance drug solubility and dissolution rate. The DSC thermograms of the pure components and optimized formulation are shown in Figure 7. The thermal parameters obtained from DSC analysis are summarized in Table 5.

X-ray Diffraction

The XRD diffractograms of the nanofiber formulation showed Dominant peaks at 2θ=21.78° (100% relative intensity) and 22.44° (45.42% relative intensity) corresponding to the characteristic diffraction planes of the semicrystalline PCL polymer lattice. The PVP K30 showed no sharp crystalline peaks, in accordance with its amorphous state. Most importantly, the characteristic peaks of pure itraconazole (9.0°, 17.4°, and 18.5° 2θ) and of pure quercetin (11.5° and 27.0° 2θ) were completely missing in the nanofiber formulation. The disappearance of the crystalline reflections of both drugs, analyzed by HighScore Plus software, is definite evidence of complete amorphization (molecular dispersion) of both drugs in the PCL/PVP matrix. This amorphous transformation is in accordance with the DSC results and is anticipated to enhance the dissolution kinetic and therapeutic bioavailability. The XRD diffraction patterns are presented in Figure 7.

Contact Angle and Wettability

The water contacts angle of the nanofiber membrane made of PCL/PVP/ITZ/QCT was 89.49±0.29°, which is a mildly hydrophilic surface (contact angle < 90°). This is a significant improvement compared to the pure PCL membranes which generally have contact angles in the range of 105°-120°. This increased hydrophilicity is because of the amphiphilic character of the PVP K30 and surface-active properties of the loaded drug molecules. The scaffold's slightly hydrophilic property is ideal for post-surgical wound dressing applications, as it allows sufficient drug elution and management of wound exudates and maintains scaffold structural integrity. The wettability of the nanofibers was evaluated by contact angle measurement (Figure 8). The contact angle values are summarized in Table 6.

Encapsulation Efficiency

For the optimized nanofiber formulation, encapsulation efficiency was repeated three times (*n*=3), to assess the reproducibility of the result. The three independent batches encapsulation efficiency is given below in Table 7. The optimized formulation had an EE of 93.95±0.38% and 92.89±0.42% (mean±SD, *n*=3) for itraconazole and quercetin, respectively, showing high drug entrapment in the nanofibers. The high encapsulation efficiency in all three batches shows that the optimized formulation is reproducible. The good encapsulation efficiency can be explained by the excellent compatibility between the drugs and the polymer matrix, which was confirmed by FTIR analysis, and by the optimized PCL:PVP ratio and the optimized electrospinning process parameters, which reduced the loss of the drug during the solvent evaporation process, allowing the incorporation of the hydrophilic drug quercetin into the hydrophilic PVP matrix and the hydrophobic drug itraconazole into the hydrophobic PCL matrix. Moreover, the experimental encapsulation efficiency was also found to be close to the predicted value by Box-Behnken Design-Response Surface Methodology (BBD-RSM) which was 93.92%, confirming the accuracy of the optimized model and the robustness of optimized formulation.

In vitro Drug Release and Release Kinetics

In vitro drug release

The *in vitro* drug release study of the optimized ITZ/QCT-loaded PCL/PVP electrospun nanofibers were repeated three times (*n*=3), and the values are represented as mean±SD. Itraconazole (ITZ) and Quercetin (QCT) showed a biphasic drug release pattern during the 8 hr evaluation period. Itraconazole release increased from 10.71±0.18% at 0.5 hr to 88.00±0.39% at 8 hr, while quercetin release increased from 12.76±0.17% to 87.50±0.31% over the same period. A small amount of initial burst release was seen in the first 2 hr, followed by a slow and controlled release up to 8 hr. The low values of SD at each sampling point suggest good

reproducibility of optimized formulation. The cumulative drug release is summarized in (Table 8).

The *in vitro* drug release study was performed in triplicate (n=3). At each sampling time, cumulative drug release was calculated and expressed as mean±Standard Deviation (SD).

Release kinetics

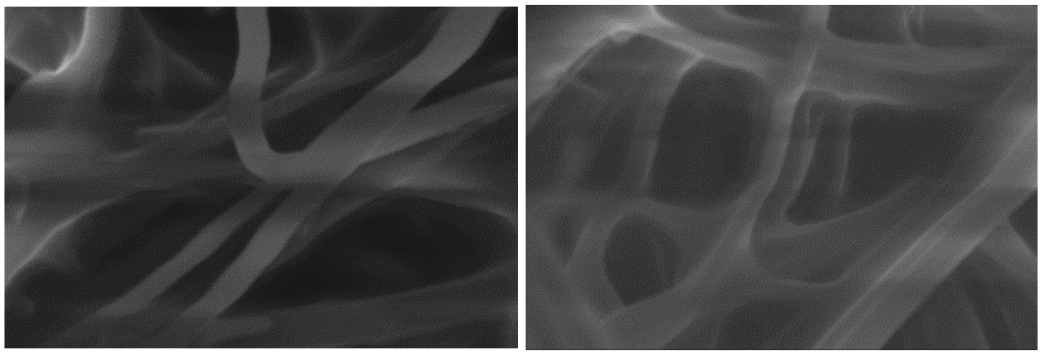
Release kinetic analysis was performed using DDSolver 1.0 by fitting the release data to Zero-order, First-order, Higuchi, and Korsmeyer-Peppas models. The cumulative drug release data obtained during the 8 hr study period were fitted to Zero-order, First-order, Higuchi, and Korsmeyer-Peppas kinetic models using

Table 8: *In vitro* cumulative drug release of Itraconazole and Quercetin from optimized nanofiber formulation.

Time (h)	ITZ Batch 1 (%CDR)	ITZ Batch 2 (%CDR)	ITZ Batch 3 (%CDR)	ITZ Mean±SD	QCT Batch 1 (%CDR)	QCT Batch 2 (%CDR)	QCT Batch 3 (%CDR)	QCT Mean±SD
0.0	0.00	0.00	0.00	0.00±0.00	0.00	0.00	0.00	0.00±0.00
0.5	10.54	10.89	10.70	10.71±0.18	12.60	12.94	12.74	12.76±0.17
1.0	20.18	20.61	20.32	20.37±0.22	23.08	23.48	23.25	23.27±0.20
2.0	36.78	37.39	37.07	37.08±0.31	38.42	39.00	38.72	38.71±0.29
3.0	50.21	50.89	50.49	50.53±0.34	50.20	50.96	50.58	50.58±0.38
4.0	61.28	61.94	60.67	61.30±0.64	60.88	61.63	61.12	61.21±0.38
5.0	70.25	71.06	70.61	70.64±0.41	69.42	70.04	69.67	69.71±0.31
6.0	77.74	78.43	78.07	78.08±0.35	76.82	77.42	77.03	77.09±0.30
7.0	82.54	83.28	82.91	82.91±0.37	82.10	82.64	82.31	82.35±0.27
8.0	87.62	88.39	87.99	88.00±0.39	87.22	87.84	87.44	87.50±0.31

Table 9: Goodness-of-fit statistics for drug release kinetic models (DDSolver 1.0).

Model	ITZ R^2	ITZ R^2adj	ITZ AIC	ITZ MSC	QCT R^2	QCT R^2adj	QCT AIC	QCT MSC
Zero-order	0.9151	0.9151	−23.76	1.94	0.8962	0.8962	−22.36	1.71
First-order	0.9163	0.9163	−23.90	1.95	0.8975	0.8975	−22.48	1.72
Higuchi	0.9679	0.9679	−33.49	2.91	0.9803	0.9803	−39.00	3.37
Korsmeyer-Peppas*	0.9918	0.9908	−45.11	4.07	0.9955	0.9949	−51.69	4.64



A. Room Temperature (25°C) – 45 Days

B. Refrigerated Condition (4–6°C) – 45 Days

Figure 9: SEM micrographs of the optimized nanofiber formulation after 45 days of storage: (a) room temperature (25°C); (b) refrigerated condition (4-6°C), showing greater structural retention at room temperature.

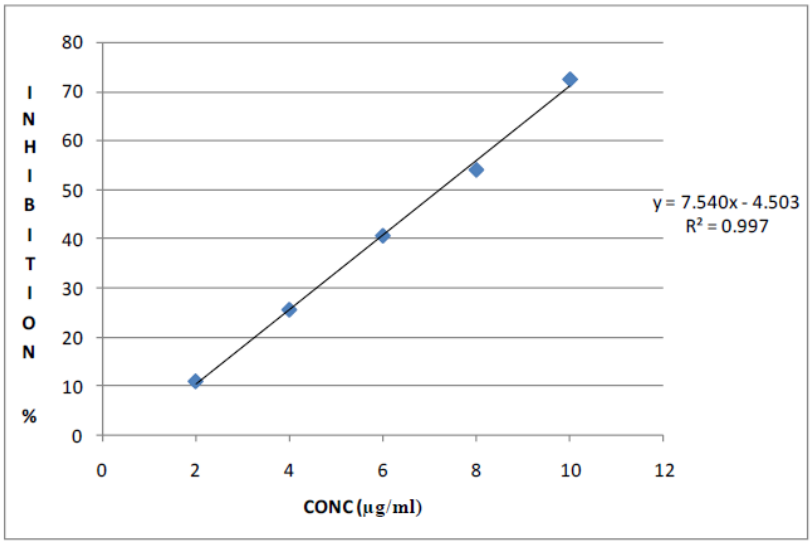


Figure 10: DPPH radical scavenging activity (% inhibition vs. concentration) of the ascorbic acid standard (2-10 µg/mL, y=7.540x – 4.503, R^2=0.997) and the ITZ/QCT-loaded nanofiber formulation (50-250 µL), the latter yielding an IC_{50} of approximately 158.3 µL.

Table 10: Physical Stability Study of Optimized Nanofibers.

Storage	Day	Appearance	Quercetin EE (%)	Itraconazole EE (%)	SEM Observation
4-6°C	0	Clear	93.35	92.89	Normal fiber morphology
4-6°C	45	Clear	92.93	91.57	Slight structural changes due to moisture
25°C	0	Clear	93.35	92.89	Normal fiber morphology
25°C	45	Clear	93.12	92.63	Fiber morphology retained; stable

Table 11: % Inhibition of DPPH radical by Ascorbic Acid (Standard) at various concentrations.

Concentration (µg/mL)	% Inhibition
2	11.1
4	25.6
6	40.6
8	53.9
10	72.3

Table 12: % Inhibition of DPPH radical by Sample PR001 at various concentrations.

Concentration (µL)	% Inhibition
50	19.44
100	33.33
150	51.38
200	62.50
250	72.22

DDSolver 1.0. Model fitting revealed that the Korsmeyer-Peppas model provided the best statistical fit for both itraconazole (R^2=0.9918, R^2adj=0.9908, AIC=−45.11, MSC=4.07) and quercetin (R^2=0.9955, R^2adj=0.9949, AIC=−51.69, MSC=4.64), as determined by the highest R^2, adjusted R^2, and MSC values alongside the lowest MSE and most negative AIC. The Higuchi model also showed good fit (ITZ: R^2=0.9679; QCT: R^2=0.9803), indicating a significant contribution of diffusion from the polymer matrix, whereas the Zero-order and First-order models demonstrated comparatively inferior fit statistics.

The release exponents (n) of 0.61 for itraconazole and 0.58 for quercetin (both between 0.45 and 0.89), confirmed a non-Fickian (anomalous) transport mechanism, which suggested that drug release had taken place by an interplay between Fickian diffusion through the PCL polymer network and polymer relaxation/swelling of the hydrophilic PVP. This mechanism is in good agreement with the composite matrix structure of the PCL: PVP system which is composed of a heterogeneous blend of PCL and PVP, in which diffusion in the hydrophobic PCL phase is slowed, and swelling of the PVP phase upon hydration gives rise to a swelling-mediated release component. The results from the goodness of fit for the kinetic models are presented in Table 9.

Best-fit model. *n*=0.61 (ITZ) and 0.58 (QCT): Non-Fickian anomalous transport.

Physical Stability Study of Quercetin-Itraconazole Loaded Nanofibers

The nanofibers were physically stable during the study period, and the appearance was very clear at both Day 0 and Day 45 under refrigerated and room-temperature conditions. The Day 45 sample was stored at room temperature and SEM results showed that there were very little structural changes in the fiber shape. However, the sample kept under refrigerated conditions exhibited slight changes in its structure, which could be due to the uptake of moisture during storage. The encapsulation efficiency slightly decreased after 45 days, suggesting good retention of quercetin and itraconazole. Overall, the room temperature storage proved to be more stable physically than the refrigerated storage. The physical stability results are presented in Table 10. The SEM images after the stability study are shown in Figure 9.

Table 13: Effect of ITZ/QCT-loaded PCL/PVP nanofibers on A431 cell viability (MTT assay, 24 hr, *n*=3, Mean±SD).

Concentration (µg/mL)	% Cell Viability (Mean±SD)	Remarks
Control (0)	100.00±5.03	Untreated baseline
100	100.08±5.62	No cytotoxicity
200	100.97±2.99	No cytotoxicity
300	92.26±3.84	Mild growth inhibition
400	68.79±3.80	Moderate cytotoxicity
500	53.91±1.75	Near IC_{50}
600	33.56±2.82	Marked cytotoxicity
700	22.26±1.56	High cytotoxicity
800	13.80±1.90	Severe cytotoxicity
900	6.63±1.10	Near-complete inhibition
1000	4.83±1.40	Near-complete inhibition

Antioxidant Activity (DPPH ASSAY)

The results of the DPPH free radical scavenging assay showed that both the standard (ascorbic acid) and the test sample (the nanofiber) exhibited concentration-dependent increases in % inhibition. Ascorbic acid showed % inhibition from 11.1% (2 µg/mL) to 72.3% (10 µg/mL) with excellent linearity ($y=7.540x-4.503$, $R^2=0.997$). The ITZ/QCT-loaded nanofiber formulation exhibited % inhibition values of 19.44%, 33.33%, 51.38%, 62.50%, and 72.22% at 50, 100, 150, 200, and 250 µL, respectively, yielding an IC_{50} of approximately 158.3 µL. The phenolic hydroxyl groups of quercetin, a well characterized free radical scavenger, are the main contributors to the Strong anti-oxidant activity that is effectively trapped in the nanofiber matrix and bioactively released. The DPPH antioxidant activity of the standard is presented in Table 11. The DPPH inhibition plots are shown in Figure 10. The antioxidant activity of the nanofiber formulation is presented in Table 12.

In vitro Cytotoxicity (MTT ASSAY)

The MTT assay against A431 cells showed the viability was significantly decreased in a time and dose dependent manner. Cytotoxicity was not seen at 100-200 µg/mL, showing good biocompatibility at sub-therapeutic doses. At 300-500 µg/mL,

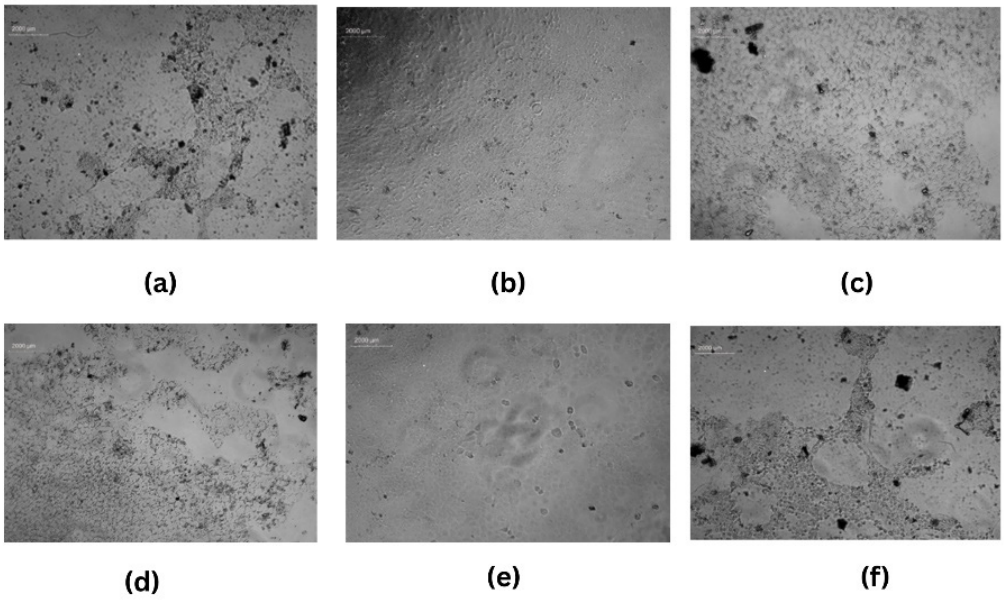


Figure 11: *In vitro* cytotoxicity of the ITZ/QCT-loaded PCL/PVP nanofiber formulation against A431 human epidermoid carcinoma cells by MTT assay (24 hr): representative cell morphology images across the tested concentration range (100-1000 µg/mL), corresponding to the dose-response data in Table (IC_{50}=520 µg/mL).

there were signs of progressive cell rounding, shrinkage of the cytoplasm, membrane blebbing and detachment, consistent with apoptosis, while at 600-1000 µg/mL there was widespread detachment and nuclear condensation consistent with advanced apoptosis/necrosis. The IC_{50} was 520 µg/mL at 24 hr, which was significantly less than that of free itraconazole (800-1200 µg/mL) and free quercetin (650-900 µg/mL), indicating an additive-to-synergistic antiproliferative effect from co-delivery. This increased cytotoxicity is believed to be due to the fact that both ITZ and QCT are released continuously, allowing for the inhibition of both the Hedgehog/angiogenic (ITZ) and the PI3K/Akt/NF-κB (QCT) pathways (Figure 11 and Table 13).

DISCUSSION

Process-Property Relationships in the Optimized Electrospinning System

Flow rate had the highest effect on all three responses in the BBD model ($p<0.0001$), which reflects the general electrospinning principle that the shear force generated by flow rate is responsible for the mass of polymer solution fed to the Taylor cone in a given amount of time and therefore, for the jet mass, the rate of solvent evaporation and the fiber diameter.[9] The high influences of PCL:PVP ratio on all three responses are associated with the solution viscosity and phase behaviour during the blend electrospinning, which have been reported in the literature to be miscible and spinnable throughout a range of PCL:PVP ratios that includes the ratios used in this study,[16] and are also biocompatible with both polymers. The dome-shaped surface of the response surface plot for EE, with peaks at high voltage and low flow rate, is in agreement with the expected decrease of residence time for the solvent evaporation and jet thinning at high voltage and low flow rate, which would in turn reduce the amount of drug diffusing out of the fiber into the surrounding bulk matrix and therefore preserve the encapsulated drug in the fiber core.

Solid-State Transformation and Drug-Polymer Compatibility

FTIR analysis did not reveal any new characteristic peaks which would signal the presence of chemical interactions between Itraconazole (ITZ) and Quercetin (QCT), confirming that there was no chemical interaction between the two drugs when they were physically incorporated into the PCL/PVP nanofiber matrix.[17] The absence of the melting endothermic peaks in DSC and crystalline peaks in XRD also suggested a conversion of both drugs from crystalline to amorphous state, probably due to hydrogen bonding between the carbonyl group of the PVP and the N-H/O-H group of the drugs in the rapid evaporation of the solvent during electrospinning.[33,34] No direct interaction between the two drugs was detected on the ITZ-QCT composite suggesting that both drugs dispersed independently in the polymer matrix. This amorphous transformation helped achieve high encapsulation efficiency (>93.95% for ITZ and >92.89% for QCT) and improved the cumulative drug release (>87.5%).

Surface Wettability and Fiber Morphology

The optimized membrane also exhibited a significantly reduced contact angle (89.49±0.29°) compared to the 105-120° which is generally reported for unmodified PCL nanofibers, in consistent with the known effect of PVP as a hydrophilic, amphiphilic co-polymer that migrates toward the surface during electrospinning, decreasing the surface energy, and electrospinning parameters and solvent selection that have also been shown to affect PCL nanofiber contact angle in a similar manner.[35] A moderately hydrophilic surface of 80°-90° is typically regarded as desirable for post-surgical wound dressings, because it allows proper wetting for drug elution and exudate absorption, but does not leave the surface too water-permeable to cause excessive swelling that may compromise the scaffold's integrity. This morphology, characterized by beads that are smooth, randomly oriented and not seen in other systems that have been electrospun, has been reported in PCL/PVP systems and has been cited as being caused by differential evaporation rates between chloroform and DMF during the jet drying process instead of drug-related defects.

Drug Release Mechanism

The optimized ITZ/QCT-loaded PCL/PVP electrospun nanofibers exhibited a reproducible biphasic drug release profile, characterized by an initial burst release followed by a controlled release during the 8 hr evaluation period. The initial burst release is attributed to the dissolution of drug molecules located near the fiber surface and the rapid hydration of the hydrophilic PVP phase, whereas the subsequent release was predominantly governed by diffusion through the hydrophobic PCL matrix. Release kinetic analysis demonstrated that the Korsmeyer-Peppas model provided the best fit for both drugs, indicating a non-Fickian (anomalous) transport mechanism involving both Fickian diffusion and polymer relaxation. These findings suggest that the optimized nanofibers provide controlled drug release suitable for localized topical delivery following skin cancer surgery. It was decided to use the 8 hr release period to represent the early post-operative period following skin cancer surgery, when the first dressing change is usually undertaken and when the risk of local recurrence and wound infection is greatest. Thus, it was more important to ensure sustained release during this timeframe than prolonged multi-day release. This helps the intended use of the nanofiber as a dress-for-surgical-wounds, as opposed to a long-term implant, in which the drug delivery can be repeated with every dressing change. However, the *in vitro* release study was carried out for only 8 hr and more studies with longer duration are needed for extended delivery of the drug.

Storage Stability

The optimized nanofibers retained acceptable morphology and encapsulation efficiency after 45 days under both refrigerated (4-6°C) and room-temperature (25°C /65±5% RH) storage conditions, with only a slight decline in encapsulation efficiency (QCT: 93.35% to 92.93% at 4-6°C and to 93.12% at 25°C /65±5% RH; ITZ: 92.89% to 91.57% at 4-6°C and to 92.63% at 25°C /65±5% RH). The stability samples were stored in airtight containers in accordance with ICH Q1A(R^2) long-term and intermediate storage recommendations. The greater structural changes observed under refrigerated conditions were most likely due to moisture condensation during repeated removal from cold storage, which may plasticize the hygroscopic PVP phase and cause local disruption of the nanofiber structure. In contrast, room-temperature storage showed better preservation of fiber morphology, suggesting that avoiding condensation-related moisture uptake is beneficial for maintaining structural integrity. For future scale-up, packaging the nanofibers in heat-sealed aluminium foil pouches with a desiccant sachet is recommended to minimize moisture exposure, particularly because of the hygroscopic nature of PVP, and to help preserve fiber integrity during storage.

Antioxidant and Cytotoxic Performance in Context

The DPPH IC_{50} value of 158.3 µL for the nanofiber formulation indicates that significant antioxidant activity of quercetin was maintained after electrospinning and encapsulation within the PCL/PVP nanofibers. The co-loaded formulation had an IC_{50} of 520 µg/mL against A431 cells, which is lower than the IC_{50} ranges of 800-1200 µg/mL for free itraconazole and 650-900 µg/mL for free quercetin individually against squamous carcinoma lines. The increased efficacy of the combined formulation over either drug alone is reminiscent of the synergistic action described for both agents alone, which include itraconazole, targeting the Hedgehog/Smoothened signaling pathway, and endothelial or tumour cell proliferation in various models of solid tumours,[18,36] and quercetin, inhibiting cell proliferation via modulation of the Bcl-2/Bax and PI3K/Akt signaling pathways in several tumour cell lines.[19] The complementary intracellular drug levels resulting from the sustained release of both agents from a single nanofiber matrix (as shown in Section 3.13) suggest a possible reason for the improved cytotoxic activity when the nanofiber matrix was loaded with both agents. In the present study, formal combination-index analysis was not performed and would be necessary to determine true synergism between the co-delivered agents.

Although cytotoxicity against normal skin cells was not evaluated in this study, previous reports suggest that the formulation is likely to have a favourable safety profile. Quercetin has been shown to produce greater cytotoxicity in cancer cells than in normal skin cells, with minimal effects on normal skin cell viability at concentrations effective against skin cancer cells.[37] Similarly, topical itraconazole nanocarrier formulations have demonstrated good local tolerability and non-irritant behaviour in skin irritation studies.[38] In addition, PCL and PVP are widely used electrospun polymers for wound dressings and are generally considered biocompatible and non-cytotoxic to keratinocytes and fibroblasts.[4] These findings indicate that the developed formulation is likely to be well tolerated by the surrounding healthy skin. However, direct cytotoxicity studies using normal skin cells and therapeutic-index evaluation are still required to confirm its safety.

Comparison with Existing Topical Delivery Systems

Unlike conventional topical carriers like liposomes, transferosomes, ethosomes, and nanoemulgels, electrospun nanofibers offer the dual advantage of drug delivery and wound dressing. While vesicular systems typically need a secondary dressing, the PCL/PVP nanofibrous mat can provide mechanical support, an ECM-like structure,[37] and sustained non Fickian drug release.[39] Both itraconazole and quercetin have been studied alone,[17,40] in the previous studies, while the current study successfully co-loaded both drugs into a single Box-Behnken-optimized PCL/PVP nanofiber. The optimized formulation exhibited high encapsulation efficiency (93.95% for ITZ and 92.89% for QCT) and the drug release was controlled for 8 hr. However, additional *ex vivo* skin permeation and *in vivo* studies are warranted to support its therapeutic efficacy and to compare its efficacy with available topical delivery systems.

STUDY LIMITATIONS AND FUTURE DIRECTIONS

There are some limitations in this study. Only the human epidermoid carcinoma (A431) cell line *in vitro* was used to assess the anticancer activity of the ITZ/QCT-loaded nanofibers while no *in vivo* tumour or wound-healing model or *ex vivo* dermal permeation was performed. Although PCL and PVP are known to be biocompatible, cytotoxicity was examined only toward A431 tumour cells, while selectivity towards normal skin cells was not evaluated and both drugs exhibit dose-dependent cytotoxicity at higher concentrations. Therefore, future studies should include normal keratinocyte or fibroblast cell lines with therapeutic index determination, along with *in vivo* post-surgical wound models and *ex vivo* human or porcine skin permeation studies to confirm the cytotoxicity, release kinetics, stability, local toxicity, skin irritation, biocompatibility, and long-term safety before translational or clinical conclusions can be drawn.

CONCLUSION

This study successfully formulated and optimized itraconazole and quercetin co-loaded PCL/PVP electrospun nanofibers for the management of skin cancer after surgery topically by Box-Behnken (BBM) response surface methodology. The optimized formulation electrospun at 17.0 kV, 0.25 mL/hr flow rate and PCL:PVP ratio of 2.29 had a fiber diameter of 389.8±35.0

nm, encapsulation efficiencies of 93.95% (ITZ) and 92.89% (QCT), and cumulative release of > 87.5% in 8 hr, with high composite desirability (D=0.927).

Amorphous solid dispersion in the nanofiber matrix was confirmed by physicochemical analysis (DSC and XRD), and there was no chemical interaction between the two drugs (FTIR) or bead-free morphology of the nanofiber matrix (SEM) which was slightly hydrophilic (contact angle 89.49°). Nanofibers were found stable for 45 days at 4-6°C and (25 °C /65±5% RH, with a slightly higher stability at room temperature than in the refrigerated state because of moisture uptake on fibers. The release was found to be non-Fickian (n=0.58-0.61), indicating the presence of both diffusion and polymer relaxation. The formulation exhibited strong cytotoxicity to A431 cells ($IC_{50=}$520 µg/mL) and antioxidant activity (DPPH IC_{50}=158.3 µL) which is greater than antioxidant activity of free drugs, which is concentration dependent.

The results indicate the dual-drug PCL/PVP nanofiber platform as a promising post-surgical drug delivery system featuring a combination of Itraconazole's anti-angiogenic, Hedgehog-inhibitory activity with Quercetin's antioxidant, pro-apoptotic effects. The next steps involve scale-up, *in vivo* wound healing, and *ex vivo* permeation studies.

ACKNOWLEDGEMENT

The authors thank the Department of Pharmaceutics, The Erode College of Pharmacy, for providing the laboratory facilities used in this study.

ABBREVIATIONS

ANOVA: Analysis of Variance; **BBD:** Box-Behnken Design; **BCS:** Biopharmaceutics Classification System; **CDR:** Cumulative Drug Release; **DMF:** Dimethylformamide; **DMSO:** Dimethyl Sulfoxide; **DPPH:** 2,2-Diphenyl-1-picrylhydrazyl; **DSC:** Differential Scanning Calorimetry; **EE:** Encapsulation Efficiency; **FBS:** Fetal Bovine Serum; **FTIR:** Fourier Transform Infrared Spectroscopy; **ITZ:** Itraconazole; **MEM:** Minimum Essential Medium; **MTT:** 3-(4,5-Dimethylthiazol-2-yl)-2,5-diphenyltetrazolium Bromide; **NCCS:** National Centre for Cell Science; **PCL:** Polycaprolactone; **PVP:** Polyvinylpyrrolidone; **QCT:** Quercetin; **RSM:** Response Surface Methodology; **SD:** Standard Deviation; **SEM:** Scanning Electron Microscopy; **XRD:** X-ray Diffraction.

CONFLICT OF INTEREST

The authors declare that there is no conflict of interest.

FUNDING

The authors declare that this research received no external funding.

ADDITIONAL STATEMENT

The authors confirm that no paper mill was used in the preparation of this manuscript and that all data were generated and analyzed by the authors.

AUTHORS CONTRIBUTION

P.P.: Conceptualization, Methodology, Writing - Original Draft. **A.S.:** Investigation, Writing - Review and Editing. **V.A.N.:** Formal Analysis, Data Curation. **S.K.:** Supervision, Project Administration. All authors approved the final manuscript.

ETHICS APPROVAL AND CONSENT

This article does not contain any studies involving human participants or animals performed by any of the authors. Consent to Participate: Not applicable. Consent for Publication: Not applicable. Clinical Trial Registration: Not applicable.

DATA AVAILABILITY STATEMENT

The datasets generated and/or analyzed during the current study are available from the corresponding author on reasonable request.

REFERENCES

1. Maleki H, Doostan M, Shojaei S, Doostan M, Stamatis H, Gkantzou E, *et al.* Nanofiber-based systems against skin cancers: therapeutic and protective approaches. J Drug Deliv Sci Technol. 2023;82:104367. doi:10.1016/j.jddst.2023.104367.
2. Leiter U, Keim U, Garbe C. Epidemiology of skin cancer: update 2019. Adv Exp Med Biol. 2020;1268:123-139. doi:10.1007/978-3-030-46227-7_6.
3. Dachani SR, Kaleem M, Mujtaba MA, Mahajan N, Ali SA, Almutairy AF, *et al.* A comprehensive review of various therapeutic strategies for the management of skin cancer. ACS Omega. 2024;9(9):10030-10048. doi:10.1021/acsomega.3c09780.
4. Tolkachjov SN, Brodland DG, Coldiron BM, Fazio MJ, Hruza GJ, Roenigk RK, *et al.* Understanding Mohs micrographic surgery: a review and practical guide for the nondermatologist. Mayo Clin Proc. 2017;92(8):1261-1271. doi:10.1016/j.mayocp.2017.04.009.
5. Huppert LA, Daud AI. Intratumoral therapies and *in situ* vaccination for melanoma. Hum Vaccines Immunother. 2022;18(1):1890512. doi:10.1080/21645515.2021.1890512.
6. Prausnitz MR, Langer R. Transdermal drug delivery. Nat Biotechnol. 2008;26(11):1261-1268. doi:10.1038/nbt.1504.
7. Elias PM. Stratum corneum defensive functions: an integrated view. J Invest Dermatol. 2005;125(2):183-200. doi:10.1111/j.0022-202X.2005.23668.x.
8. Hadgraft J. Skin, the final frontier. Int J Pharm. 2001;224(1-2):1-18. doi:10.1016/S0378-5173(01)00789-2.
9. Bhardwaj N, Kundu SC. Electrospinning: a fascinating fiber fabrication technique. Biotechnol Adv. 2010;28(3):325-347. doi:10.1016/j.biotechadv.2010.01.004.
10. Ramakrishna S, Fujihara K, Teo WE, Yong T, Ma Z, Ramaseshan R. Electrospun nanofibers: solving global issues. Mater Today. 2006;9(3):40-50. doi:10.1016/S1369-7021(06)71389-X.
11. Xie J, Li X, Xia Y. Putting electrospun nanofibers to work for biomedical research. Macromol Rapid Commun. 2008;29(22):1775-1792. doi:10.1002/marc.200800381.
12. Yang Y, Zhang R, Liang Z, Guo J, Chen B, Zhou S, *et al.* Application of electrospun drug-loaded nanofibers in cancer therapy. Polymers (Basel). 2024;16(4):504. doi:10.3390/polym16040504.
13. Charernsriwilaiwat N, Opanasopit P, Rojanarata T, Ngawhirunpat T, Supaphol P. Preparation and characterization of chitosan-hydroxybenzotriazole/polyvinyl alcohol blend nanofibers by the electrospinning technique. Carbohydr Polym. 2010;81(3):675-680. doi:10.1016/j.carbpol.2010.03.031.
14. ScienceDirect Topics. Polycaprolactone — an overview [Internet]. Amsterdam: Elsevier; 2024 [cited 2024 Apr 19]. Available from: https://www.sciencedirect.com/topics/medicine-and-dentistry/polycaprolactone
15. Paczkowska-Walendowska M, Ignacyk M, Miklaszewski A, Plech T, Karpiński TM, Kwiatek J, *et al.* Electrospun nanofibers with pomegranate peel extract as a new

concept for treating oral infections. Materials (Basel). 2024;17(11):2558. doi:10.3390/ma17112558.

16. Kim GM, Le KH, Giannitelli SM, Lee YJ, Rainer A, Trombetta M. Electrospinning of PCL/PVP blends for tissue engineering scaffolds. J Mater Sci Mater Med. 2013;24(6):1425-1442. doi:10.1007/s10856-013-4893-6.
17. Viscusi G, Paolella G, Lamberti E, Caputo I, Gorrasi G. Quercetin-loaded polycaprolactone-polyvinylpyrrolidone electrospun membranes for health application: design, characterization, modeling and cytotoxicity studies. Membranes (Basel). 2023;13(2):242. doi:10.3390/membranes13020242.
18. Jin S, Liu X, Cai L, Yan J, Li L, Dong H, *et al.* Itraconazole promotes melanoma cells apoptosis via inhibiting hedgehog signaling pathway-mediated autophagy. Front Pharmacol. 2025;16:1545243. doi:10.3389/fphar.2025.1545243.
19. Ranganathan S, Halagowder D, Sivasithambaram ND. Quercetin suppresses Twist to induce apoptosis in MCF-7 breast cancer cells. PLoS One. 2015;10(10):e0141370. doi:10.1371/journal.pone.0141370.
20. Aghababaei F, Hadidi M. Recent advances in potential health benefits of quercetin. Pharmaceuticals (Basel). 2023;16(7):1020. doi:10.3390/ph16071020.
21. Lee JH, Park C, Weon KY, Kang CY, Lee BJ, Park JB. Improved bioavailability of poorly water-soluble drug by targeting increased absorption through solubility enhancement and precipitation inhibition. Pharmaceuticals (Basel). 2021;14(12):1255. doi:10.3390/ph14121255.
22. Wang Z, Zou W, Liu L, Wang M, Li F, Shen W. Characterization and bacteriostatic effects of β-cyclodextrin/quercetin inclusion compound nanofilms prepared by electrospinning. Food Chem. 2021;338:127980. doi:10.1016/j.foodchem.2020.127980.
23. Srivastava N, Bansal A, Aggarwal K, *et al.* Development and validation of UV spectrophotometric method for the quantitative estimation of quercetin in bulk followed by its solubility studies. J Appl Spectrosc. 2024;91:700-708. doi:10.1007/s10812-024-01773-1.
24. Badawi AA, El-Nabarawi MA, El-Setouhy DA, Alsammit SA. Formulation and stability testing of itraconazole crystalline nanoparticles. AAPS PharmSciTech. 2011;12(3):811-820. doi:10.1208/s12249-011-9651-9.
25. Yu DG, Wang X, Li XY, Chian W, Li Y, Liao YZ. Electrospun biphasic drug release polyvinylpyrrolidone/ethyl cellulose core/sheath nanofibers. Acta Biomater. 2013;9(3):5665-5672. doi:10.1016/j.actbio.2012.10.021.
26. Kokalj Ladan M, Straus J, Tavčar Benković E, Kreft S. FT-IR-based method for rutin, quercetin and quercitrin quantification in different buckwheat (*Fagopyrum*) species. Sci Rep. 2017;7(1):7226. doi:10.1038/s41598-017-07665-z.
27. Elzein T, Nasser-Eddine M, Delaite C, Bistac S, Dumas P. FTIR study of polycaprolactone chain organization at interfaces. J Colloid Interface Sci. 2004;273(2):381-387. doi:10.1016/j.jcis.2004.02.001.
28. Salim SA, Badawi NM, El-Moslamy SH, Kamoun EA, Daihom BA. Novel long-acting brimonidine tartrate loaded-PCL/PVP nanofibers for versatile biomedical applications: fabrication, characterization and antimicrobial evaluation. RSC Adv. 2023;13(22):14943-14957. doi:10.1039/d3ra02244g.
29. Hussain S, Malik NS, Tulain UR, Erum A, Mahmood A, Akram S, *et al.* Itraconazole-loaded polycaprolactone nanoparticle gel for enhanced transdermal delivery: development, characterization, and *ex vivo* evaluation. Int J Nanomedicine. 2025;20:15655-15681. doi:10.2147/IJN.S560741.
30. Paczkowska-Walendowska M, Rosiak N, Plech T, Karpiński TM, Miklaszewski A, Witkowska K, *et al.* Electrospun nanofibers loaded with marigold extract based on PVP/HPβCD and PCL/PVP scaffolds for wound healing applications. Materials (Basel). 2024;17(8):1736. doi:10.3390/ma17081736.
31. Langwald SV, Ehrmann A, Sabantina L. Measuring physical properties of electrospun nanofiber mats for different biomedical applications. Membranes (Basel). 2023;13(5):488. doi:10.3390/membranes13050488.
32. Okonogi S, Kaewpinta A, Chaijareenont P. Stability and influence of storage conditions on nanofibrous film containing tooth whitening agent. Pharmaceutics. 2021;13(4):449. doi:10.3390/pharmaceutics13040449.
33. Li XY, Li YC, Yu DG, Liao YZ, Wang X. Fast disintegrating quercetin-loaded drug delivery systems fabricated using coaxial electrospinning. Int J Mol Sci. 2013;14(11):21647-21659. doi:10.3390/ijms141121647.
34. Stoyanova N, Spasova M, Manolova N, Rashkov I, Georgieva A, Toshkova R. Quercetin- and rutin-containing electrospun cellulose acetate and polyethylene glycol fibers with antioxidant and anticancer properties. Polymers (Basel). 2022;14(24):5380. doi:10.3390/polym14245380.
35. Tiyek I, Gunduz A, Yalcinkaya F, Chaloupek J. Influence of electrospinning parameters on the hydrophilicity of electrospun polycaprolactone nanofibres. J Nanosci Nanotechnol. 2019;19(11):7251-7260. doi:10.1166/jnn.2019.16605.
36. Choi CH, Ryu JY, Cho YJ, Jeon HK, Choi JJ, Ylaya K, *et al.* The anti-cancer effects of itraconazole in epithelial ovarian cancer. Sci Rep. 2017;7(1):6552. doi:10.1038/s41598-017-06510-7.
37. Doroshenko KM, Shevchenko ON. Transferosomes as advanced nanocarriers for enhanced drug delivery in skin cancer therapy: a comprehensive review. Appl Biochem Biotechnol. 2026;198:2219-2256. doi:10.1007/s12010-025-05498-5.
38. Rédai EM, Péterfi O, Gergely AL, Barabás E, Pintea A, Antonoaea P, *et al.* Production, characterization, and *in vitro* antifungal evaluation of itraconazole-loaded fibrous sheets prepared by electrospinning with a factorial design. Appl Sci. 2025;15(2):710. doi:10.3390/app15020710.
39. Paliwal S, Sundaram J, Mitragotri S. Induction of cancer-specific cytotoxicity towards human prostate and skin cells using quercetin and ultrasound. Br J Cancer. 2005;92:499-502. doi:10.1038/sj.bjc.6602364.
40. Patil AS, Chougale SS, Kokatanr U, Hulyalkar S, Hiremath RD, Japti V, Masareddy R. Formulation and evaluation of itraconazole-loaded nanoemulgel for efficient topical delivery to treat fungal infections. Ther Deliv. 2024;15(3):165-179. doi:10.4155/tde-2023-0062.

Cite this article: Palanisamy P, Shanmugham A, Narayana VA, Kumar S. Fabrication and Optimization of Dual Drug-Loaded Itraconazole-Quercetin PCL/PVP Electrospun Nanofibers for Post-Surgical Skin Cancer Therapy. Indian J of Pharmaceutical Education and Research. 2027;61:10.5530/ijper.20270038.